Downloaded from orbit.dtu.dk on: Nov 14, 2024

DTU Library

A Quantitative Comparison of Aeroelastic Computations using Flex5 and Actuator Methods in LES

Hodgson, E L; Andersen, S J; Troldborg, N; Forsting, A Meyer; Mikkelsen, R F; Sørensen, J N

Published in:
Journal of Physics - Conference Series

Link to article, DOI:
10.1088/1742-6596/1934/1/012014

Publication date:
2021

Document Version
Publisher's PDF, also known as Version of record

Link back to DTU Orbit

Citation (APA):
Hodgson, E. L., Andersen, S. J., Troldborg, N., Forsting, A. M., Mikkelsen, R. F., & Sørensen, J. N. (2021). A Quantitative Comparison of Aeroelastic Computations using Flex5 and Actuator Methods in LES. *Journal of Physics - Conference Series*, *1934*, Article 012014. https://doi.org/10.1088/1742-6596/1934/1/012014

General rights
Copyright and moral rights for the publications made accessible in the public portal are retained by the authors and/or other copyright owners and it is a condition of accessing publications that users recognise and abide by the legal requirements associated with these rights.

- Users may download and print one copy of any publication from the public portal for the purpose of private study or research.
- You may not further distribute the material or use it for any profit-making activity or commercial gain
- You may freely distribute the URL identifying the publication in the public portal

If you believe that this document breaches copyright please contact us providing details, and we will remove access to the work immediately and investigate your claim.

Journal of Physics: Conference Series

PAPER • **OPEN ACCESS**

A Quantitative Comparison of Aeroelastic Computations using Flex5 and Actuator Methods in LES

To cite this article: E L Hodgson *et al* 2021 *J. Phys.: Conf. Ser.* **1934** 012014

View the article online for updates and enhancements.

The Electrochemical Society
Advancing solid state & electrochemical science & technology

The ECS is seeking candidates to serve as the
Founding Editor-in-Chief (EIC) of ECS Sensors Plus,
a journal in the process of being launched in 2021

The goal of ECS Sensors Plus, as a one-stop shop journal for sensors, is to advance the fundamental science and understanding of sensors and detection technologies for efficient monitoring and control of industrial processes and the environment, and improving quality of life and human health.

Nomination submission begins: May 18, 2021

This content was downloaded from IP address 89.23.224.68 on 15/06/2021 at 10:51

A Quantitative Comparison of Aeroelastic Computations using Flex5 and Actuator Methods in LES

E L Hodgson[1], S J Andersen[1], N Troldborg[2], A Meyer Forsting[2], R F Mikkelsen[1], J N Sørensen[1]

[1] Technical University of Denmark, Department of Wind Energy, Anker Engelunds Vej 1, 2800 Kgs Lyngby, Denmark
[2] Technical University of Denmark, Department of Wind Energy, Frederiksborgvej 399, 4000 Roskilde, Denmark

E-mail: emlh@dtu.dk

Abstract. Actuator disc and actuator line techniques are widely used for modelling wind turbines operating in wind farms. These techniques essentially replace the blade geometry with applied body forces, which reduce the resolved length scales significantly and hence the required grid resolution. This work is a verification of the coupling between the flow solver EllipSys3D and the aeroelastic tool Flex5, through a quantitative comparison of coupled actuator line, coupled actuator disc, and standalone Flex5. Steady state performance predictions, instantaneous reaction to turbulence and damage equivalent load analyses all show a very good agreement between the three methods. Differences can be explained primarily by the higher fidelity modelling of the coupled simulations; this is particularly in regard to the influence of blade flexibility, as the actuators deflect and interact with the modelled flow. Additionally, some overpredictions of loading at the blade tip and root below rated velocity for the actuator methods can be attributed to the Gaussian smearing used to apply the body forces.

1. Introduction

The effective planning of large wind farms requires accurate and reliable numerical tools to both assess the achievable power output and predict component fatigue. Real wind farms experience instantaneous variations in wind speed, yaw, shear and turbulence. The turbine wakes are also highly turbulent including large scale motions, e.g. wake meandering, which has been shown to cause a noticeable increase in the fatigue loading of subsequent turbines [1]. Investigating these time-varying effects requires turbulence resolving numerical simulations which can adequately capture important wake structures. However, as demonstrated by Sørensen *et al.* [2], the spatial and temporal discretisation that would be required to directly resolve all scales relevant to an entire wind farm is beyond current computing capabilities.

Reducing the required grid resolution can be achieved using actuator disc (AD) or actuator line (AL) techniques to replace the actual turbine blade geometry with applied body forces, and is widely used in Large Eddy Simulation (LES) to study wakes and wind farm flows [2-4]. The actuator disc (AD) method distributes the forces over the entire rotor swept area, and hence the influence of the blades is modelled as an integrated quantity in the azimuthal direction. The

Content from this work may be used under the terms of the Creative Commons Attribution 3.0 licence. Any further distribution of this work must maintain attribution to the author(s) and the title of the work, journal citation and DOI.
Published under licence by IOP Publishing Ltd

actuator line (AL) method, developed by Sørensen and Shen [5], overcomes the limitations of the actuator disc by distributing the body forces along rotating radial lines representing the blades. This allows more detailed studies of wake dynamics, including tip vortices and their effects on the induced velocity in the rotor plane, however resolving the blade motion requires a much smaller timestep than can be used for actuator disc. The actuator body forces are generally obtained using BEM-based methods with airfoil data as input, including aeroelastic tools.

The aim of the present work is to provide a consistent verification of the coupling between the EllipSys3D flow solver, which conducts large eddy simulations employing actuator methods, and the aeroelastic tool Flex5 through which the body forces are calculated. It will be achieved primarily through a quantitative comparison between standalone Flex5, coupled AD-Flex5, and coupled AL-Flex5. Through investigation of the differences across a variety of operational scenarios, this work also intends to demonstrate the advantages and limitations of the methods. Other works have performed comparisons of AD and AL [6,7], or verification of coupling frameworks for other solvers [8,9]; two studies validating the coupling between an LES CFD solver and an aeroelastic tool are Sprague *et al.* [10] between Nalu-Wind and OpenFAST, and Krüger *et al.* [8] between PALM and FAST. The EllipSys3D-Flex5 coupling has been utilized in several previous works [2, 11, 12], but the present work is the first specifically to verify the coupling. Additionally, this work compares the two actuator methods particularly regarding loading predictions and turbine performance, uses a larger, more flexible turbine to consider the influence of flexibility, and includes results from turbulent simulations.

The paper is organised into the following five sections: Introduction; Methodology, in which Flex5, EllipSys3D and the coupling between them are described; Simulation Setup; Results, in which the verification is presented and discussed; and Conclusions.

2. Methodology

2.1. Flex5

The aeroelastic tool Flex was originally developed by Øye [13] at the Technical University of Denmark (DTU), and is widely used in industry. The current implementation of the tool, Flex5, has 28 degrees of freedom, and uses the joint coordinates approach and the Rayleigh-Ritz approximation to set equations of motion [14]. The reduced set of DOFs that these approaches provide give an advantage of computational speed, while capturing the major deflection modes. However, the reliance on thin beam and small deflection assumptions means that non-linear effects are not captured. For a detailed description of the framework and formulation of Flex5, see Branlard [14].

Flex5 has a built in aerodynamics module which uses the blade element momentum method to calculate aerodynamic forces, based on tabulated two-dimensional aerofoil data. The Shen tip correction [15] was employed for this work. Flex5 also includes schemes for dynamic stall, tower shadow, and a dynamic wake model which applies a temporal filter on the induced velocity to accurately capture the behaviour in time of blade loading due to dynamic changes in thrust.

2.2. EllipSys3D

EllipSys3D is a three-dimensional, incompressible, multiblock Navier-Stokes solver, developed in close collaboration between the former Risø [16] and DTU [17]. The governing equations in conservative form are expressed in general curvilinear coordinates in a collocated grid arrangement, and solved using a finite volume method. The solver is formulated in primitive variables (pressure and velocity), and for this study the pressure correction equation was evaluated using the SIMPLE algorithm with Rhie-Chow interpolation to avoid pressure decoupling. Discretisation and evaluation of the convective terms was achieved with a hybrid scheme which switches between a fourth order Central Differencing scheme and the third-order QUICK scheme based on a suitable limiter function as described by Strelets [18]. The simulations

are advanced in time using a second-order accurate three-level implicit time-stepping method which relies on sub iterations at each individual time step.

Large Eddy Simulations apply a low-pass filter to the Navier-Stokes equations, and hence represents the velocity as a sum of the filtered velocity and the small scales. The filtered velocity is explicitly simulated, whereas the smaller scales are modelled by a sub-grid scale (SGS) model, which also provides closure. The SGS model by Deardorff [19] was employed for these simulations. The actuator disc and actuator line methods are used in EllipSys3D for wind turbine modelling, as implemented by Mikkelsen [20] and Troldborg [3], and these are coupled to the Flex5 aeroelastic solver [2].

2.3. Coupling

EllipSys3D, Flex5, and the coupling between them are written in Fortran, with the majority of data transfer modules common to both the actuator disc and actuator line implementations. The coupling has a loose numerical approach for time stepping, meaning that the data transfer and update only occur on every time increment, and not within the sub iterations of the flow solver. The choice of loose over strong coupling is appropriate and provides a sufficiently stable solution [21]. If the timestep in EllipSys3D is larger than that of Flex5, Flex5 will conduct several timesteps based on the velocity field of one EllipSys3D timestep, in which the blade positions are updated and the flow velocities extracted from different positions in the same stationary LES field. The time-stepping procedure is as follows:

(i) EllipSys3D locates the mesh cells corresponding to the deflected blade positions provided by Flex5 in the previous timestep, and uses trilinear interpolation to calculate the velocity components along them;

(ii) Flex5 receives these velocity components and converts them into its own coordinate system;

(iii) Flex5 conducts its main loop over the timestep, using the velocity components to calculate blade loads and deflections from BEM theory and tabulated aerofoil data;

(iv) Flex5 transforms the updated deflected blade positions and loads to the EllipSys3D coordinate system;

- In cases where the Flex5 timestep is smaller than that of EllipSys3D, operations i) to iv) will be repeated for each Flex5 timestep to compute new loads and deflected positions within the same LES field until the full EllipSys3D timestep is completed;
- In the AD, an extra step computes an average loading per unit area from all Flex5 steps within the EllipSys3D timestep, which is then distributed over a sector for each blade, i.e. three sectors of 120 degrees; in AL, deflections and loads from the final (or only) Flex5 timestep are used by EllipSys3D;

(v) EllipSys3D updates the actuator positions and body forces accordingly; to avoid singularities, forces are smeared with a Gaussian distribution using a regularisation kernel. This is the case for both actuator disc and actuator line in the current implementation of the coupling.

This coupling allows the flow solver to account for both the loads and the fully deflected blade positions in the wind turbine model, which are themselves derived from the velocity components obtained from solving the Navier-Stokes equations.

3. Simulation Setup

3.1. DTU10MW RWT

The DTU10MW reference wind turbine (RWT) was chosen for this work due to the larger radius and blade flexibility making it more relevant to modern offshore wind turbines than older and

smaller turbine models. A detailed description is available in [22], but key features are: rotor diameter of 178.3m; cut in, rated and cut out wind speed of 4, 11.4 and 25m/s respectively; 10MW rated power; shaft tilt of 5°; precone of -2.5°; and a rotor prebend of 3.332m. When investigating the influence of flexibility, the 'stiff' scenario has all DOFs except those of shaft rotation and torsion deactivated, while 'flexible' has all DOFs activated.

All simulations were conducted without gravity, ground or shear. Throughout, for both Flex5 standalone and coupled actuator methods, the Shen tip correction was used with constants of $c_1 = -0.125$ and $c_2 = 30.0$. Air was modelled with a density of 1.22 kgm^{-3} and a dynamic viscosity of 1.769 x 10^{-5} kgm^{-1}.

3.2. Turbulence

Artificial turbulent fluctuations can be generated using the Mann spectral model [23, 24], which is based on a linearisation of the Navier-Stokes equations and uses rapid distortion theory to model the spectral tensor. The generated turbulence field contains turbulent velocity components for all three coordinate directions, which are Gaussian, anisotropic, homogeneous and stationary, with second order statistics matched to the neutral atmosphere. Taylor's frozen flow hypothesis is employed to link the streamwise spatial dimension with time, and the length of the box mitigates temporal periodicity. The turbulent fluctuations were applied as body force fluctuations over a plane 5R upstream of the rotor (see Gilling *et al.* [25] for implementation details). A Mann box with parameters $\alpha\epsilon = 0.07, \gamma = 3, L = 29.4$, and dimensions 8R x 8R x 1030R was used, which resulted in an average turbulence intensity of 9%.

3.3. Computational Domain

Throughout, the overall domain size was 25R x 25R x 25R. Simulations without turbulence had an equidistant region of 2R x 2R x 2R, centred around the rotor; for the turbulent studies, the equidistant region was 10R x 4R x 4R (extending 6R in front of the rotor and 4R behind). As the turbulence was applied 5R upstream of the rotor, the extension of the equidistant region in all coordinate directions ensured that the applied turbulence was not distorted by a changing grid size in front of or close to the turbine position. Figure 1 shows the mesh and domain setup, with example planes of velocity magnitude in green (whole domain streamwise plane) and blue (2R in front of the turbine), and the position of turbulence application in red.

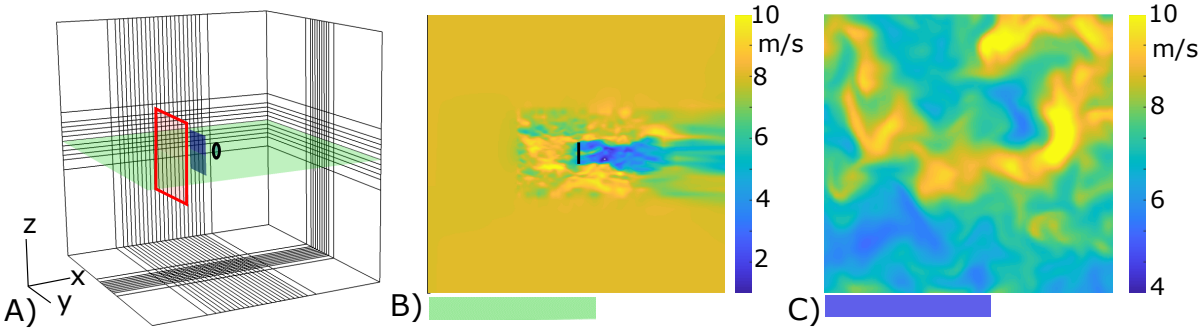

Figure 1. Domain setup: A) domain (every 8th line shown for clarity), red square shows turbulent body forces application, black circle shows turbine position; B) velocity magnitude over green plane for AD simulation; C) velocity magnitude over blue plane.

The timestep was 0.2s for AD simulations in order to satisfy the CFL number condition, and 0.02s for AL, to ensure that the lines did not move more than one cell per timestep. In Flex5, the timestep of 0.02s is the largest possible while still resolving the structural eigenfrequencies,

and hence in AL there was no repeated Flex5 calculation in the coupling as the timesteps are identical (note that this is not a requirement). Although the AD had a timestep 10 times greater, the advantage in overall simulation time was not as large, as the AD simulations were only around 4.5 times faster. This means that even despite the very high speed of the individual aeroelastic computations, conducting many for each EllipSys3D timestep can act as a bottleneck to the overall simulation time.

3.4. Grid Study

A grid study was conducted to provide the required spatial refinement to achieve grid independence in the coupled EllipSys3D - Flex5 simulations. Figure 2 shows the convergence of the thrust coefficient CT for both coupled actuator methods, based on the percentage difference from the result at the finest grid size (64 mesh points per radius).

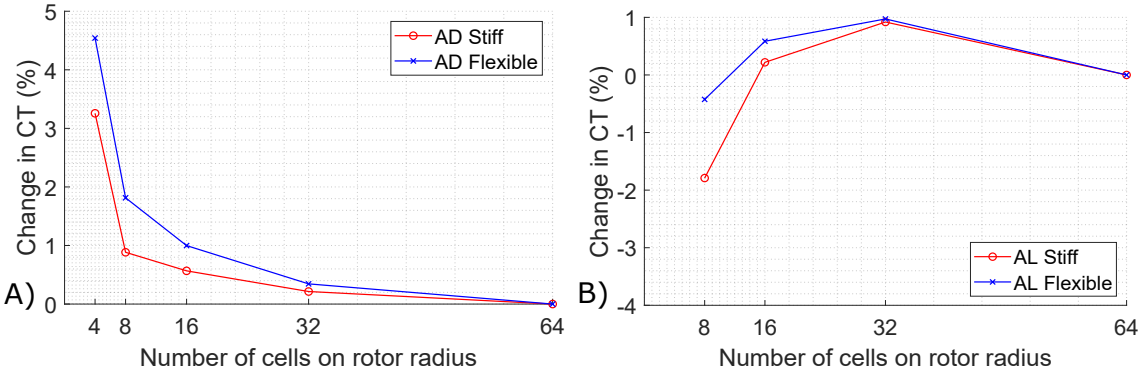

Figure 2. Grid Study using CT: A) EllipSys3D - AD; B) EllipSys3D - AL

Both actuator methods show a change in CT of less than 1% between using 16 or 64 mesh points on the rotor radius, for either a fully stiff or fully flexible turbine. Therefore, the 16 mesh point radius was chosen as an appropriate resolution for all simulations. However, it should be noted that this resolution will not result in resolved tip vortices in the case of actuator lines, see Troldborg [3]. The coupling for both AL and AD involves Gaussian smearing of forces, as described above; throughout this work the regularisation parameter $\epsilon = 3.0\Delta r$ was used (Δr equals the cell length in the equidistant region). As described in Meyer Forsting and Troldborg [26], the poorer convergence of the AL is caused by maintaining $\epsilon = 3.0\Delta r$ throughout the grid study, as it results in an increased error in the angle of attack estimation at higher blade discretisations.

The grid study was conducted using the convergence of an integrated quantity, CT, with steady-state operation at below rated velocity. However, this work aims to verify the coupling across all operational velocities, and also in turbulent conditions where dynamic changes are important. Therefore, the choice of 16 mesh points per radius was informed by the grid study, but also by practicalities of computational cost. Wind farm studies using actuator discs frequently use a significantly lower radial discretisation of 3-4 mesh points per radius [27, 28]; with the setup and grid study conducted here, this would result in a 3.2% difference in CT compared to the 64 point mesh radius case. In the actuator line wind farm study by Andersen [29], 17 points per line was used. The choice to use 16 points for this work intends to provide a useful comparison between the two methods and be computationally realistic.

4. Results

4.1. Steady State Performance

Steady state performance was assessed using a velocity ramp covering the range 5m/s - 25m/s, with an increment of 1m/s every 100s. Figure 3 shows the velocity input to the turbine controller (A), and the induction in the coupled simulations (B). Note that in Figure 3B, the increasing velocity close to the rotor plane is a result of excluding the turbine nacelle. For all graph notations, Flex5 standalone is referred to as 'Flex5', coupled Flex5-EllipSys3D AD as 'AD', and coupled Flex5-EllipSys3D AL as 'AL'.

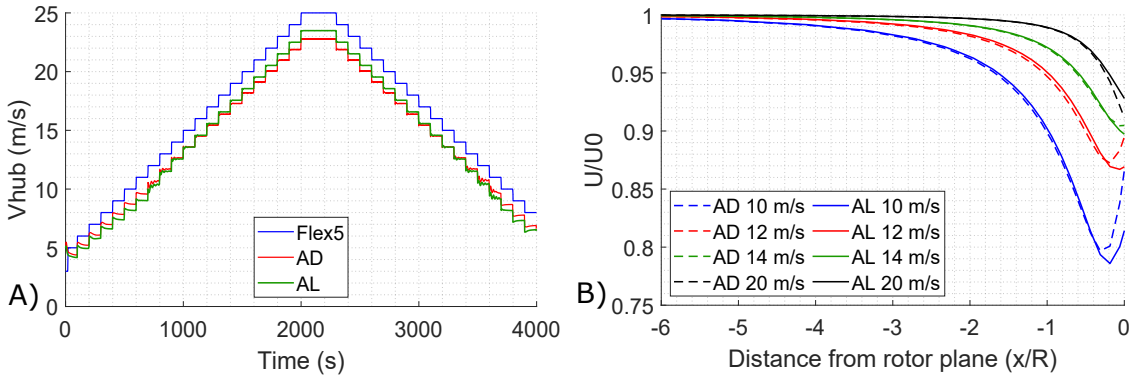

Figure 3. A) Measured Vhub; B) Flow induction towards rotor plane

The velocity used in the standalone Flex5 turbine controller exactly mirrors the input ramp, as it is taken directly from the input velocity. For the actuator simulations, the controller input is a filtered velocity taken from the rotor centre, which includes the effects of both flow induction and the acceleration through the nacelle gap. Figure 3B shows very good agreement between the induction for the two actuator methods until 0.4R upstream of the rotor. After this, close to the rotor plane, the difference in induction is due to the thrust coefficient, rather than error arising from distributing forces over a disc or a line, as shown in Meyer Forsting [30]. The difference in measured velocity at the rotor plane may result in different turbine responses between the actuator methods, as this is the value used in the controller.

The steady state performance was assessed by averaging each quantity over the final 25s of each 100s interval to ensure a steady state had been reached. The main performance curves generated from the velocity ramp are shown in Figure 4. Note that quantities are plotted against the inflow windspeed, not the measured Vhub shown in Figure 3A.

All four graphs in Figure 4 effectively collapse to a single curve after surpassing the rated velocity of 11.4m/s, and in general show good agreement between the methods. However, differences are present below and around rated velocity, most notably in CP; at 10m/s flexible AD and flexible AL are 6% and 12% higher than Flex5, respectively. Additionally, the actuator methods have a smaller region of zero pitch (7-11m/s for Flex5, 8-11m/s for AD, and 9-10m/s for AL); these differences may arise from the induction, and from where the velocity used by the controller is measured.

The impact of flexibility is negligible for Flex5 standalone, but much more visible in the coupled simulations. For AD and AL below rated, the stiff turbines have a higher CP and CT than the flexible equivalent; also, between 10m/s - 12m/s when rated velocity is reached, the stiff turbines start pitching earlier and show an earlier reduction in CT. Unlike in a purely BEM-based tool where the blades do not interact with the flow, coupling with a flow solver results in a turbine which is modelled inside a solved flow and hence can interact with it. Hence,

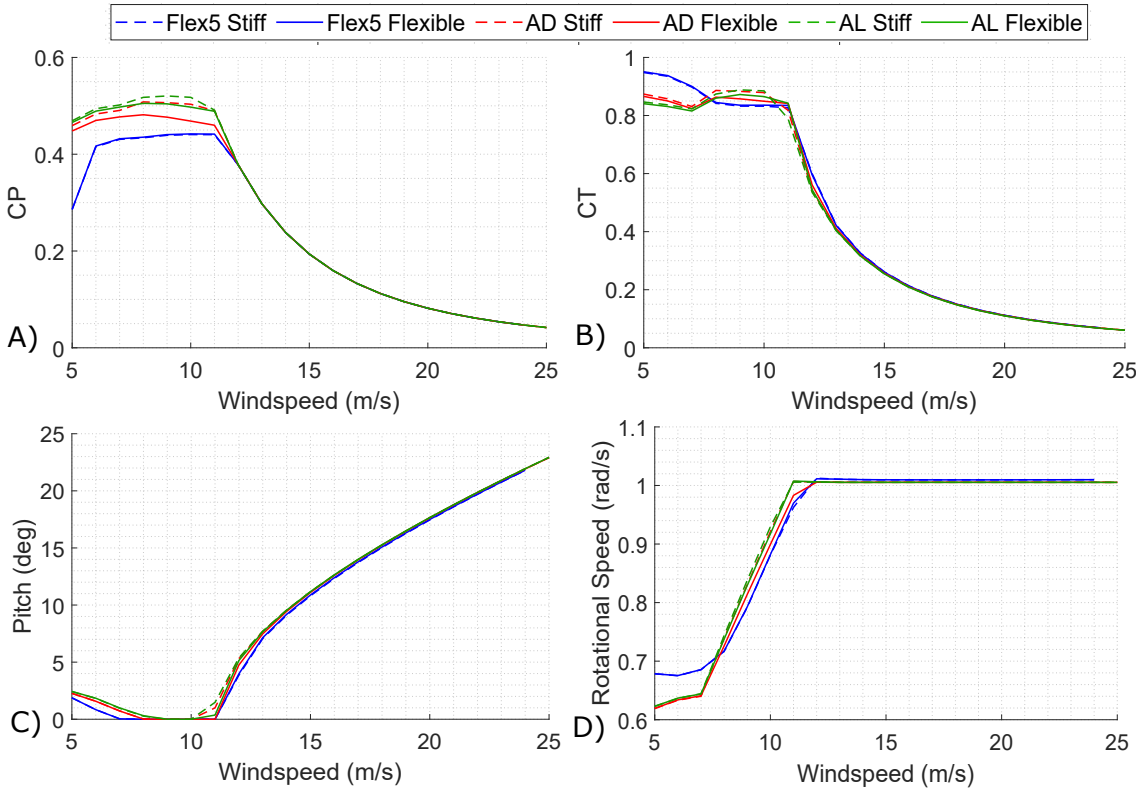

Figure 4. Steady state performance: A) Power coefficient CP; B) Thrust coefficient CT; C) Pitch angle; D) Rotational Speed

the differences arising from stiffness are larger for the actuator methods, particularly with large and highly flexible turbine blades such as those of the DTU10MW RWT.

Figure 5 further illustrates the differences between flexible and stiff actuator simulations by presenting the mean normalised blade loads at 10m/s. The means were calculated by averaging the loads over all timesteps of a full rotor revolution when the turbine was operating in steady state, and over all three blades.

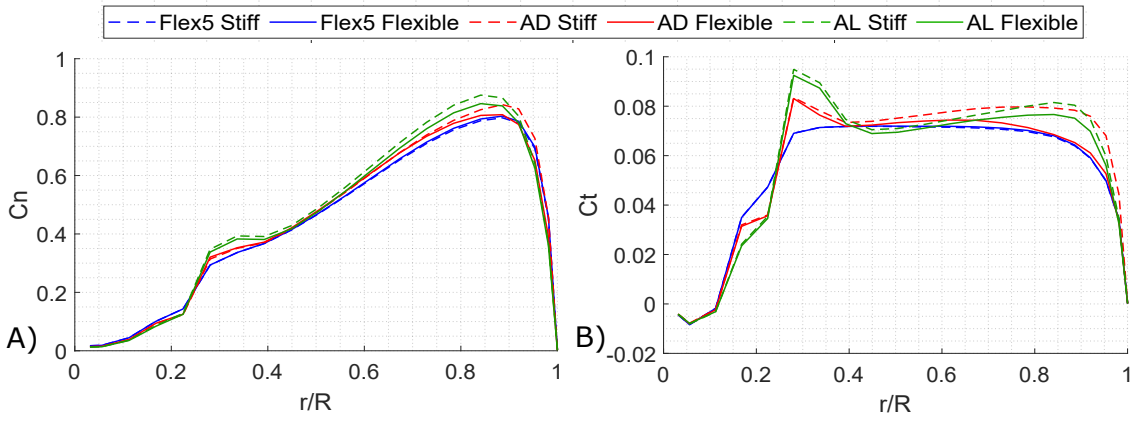

Figure 5. Normalised mean blade loads, U = 10m/s: A) normal; B) tangential

Note that this windspeed was chosen in order to demonstrate the largest discrepancies, which occur at the thrust peak just before the controller introduces pitching and hence where the blade loading is highest. At higher windspeeds where the blade is deloaded by pitch control, the difference between both stiff and flexible turbines and between the three simulation methods becomes almost negligible, showing very good agreement.

Imposing stiffness in the coupled actuator simulations causes a increased loading, especially towards the blade tip. The tangential loading prediction for the actuator disc decreases by 20% at 90% radius with the inclusion of blade flexibility, which could be due to the flexibility acting over the entire rotor plane rather than just smeared over lines as in AL. Further work will investigate the implications of this flexible implementation of the actuator disc, and whether these discrepancies around rated occur regardless of blade discretisation.

Aside from the influence of flexibility, comparing the actuator methods with Flex5 standalone shows clear differences at the blade tip and root, which may also contribute to the differences in CP and CT seen below rated velocity. For all except the flexible actuator disc, the loading is predicted higher at the blade tip than by standalone Flex5; for flexible AL this is 3% and 15% at 90% radius for normal and tangential respectively. Additionally, a peak in tangential loading at 27% radius for the actuator methods corresponds to the point of maximum chord. As demonstrated by Dağ and Sørensen [31] and Meyer Forsting *et al.* [32], the Gaussian smearing used to apply the actuator body forces to a coarse computational grid can cause this overprediction. The smearing means a viscous core is formed in the released vorticity, hence reducing the velocity induction at the blade and increasing the loading [32]. Implementing the proposed tip correction [33] in the Flex5-EllipSys3D coupling is likely to reduce this difference.

4.2. Turbulence and Damage Equivalent Loads

Two velocities, 8m/s and 12m/s, were chosen for the turbulent simulations, i.e. below and just above the rated wind speed. The Mann box gave a turbulence intensity of around 9%, and all simulations were run for 3900s. In the coupled EllipSys3D simulations, the turbulent fluctuations were applied 5R upstream of the rotor; in Flex5 standalone, where the flow itself is not directly solved, the turbulent velocity is applied directly at the turbine. This is a legitimate approach to compare overall statistics, but instantaneous changes can only be directly compared between the actuator methods. Figure 6, below, shows power variation against time.

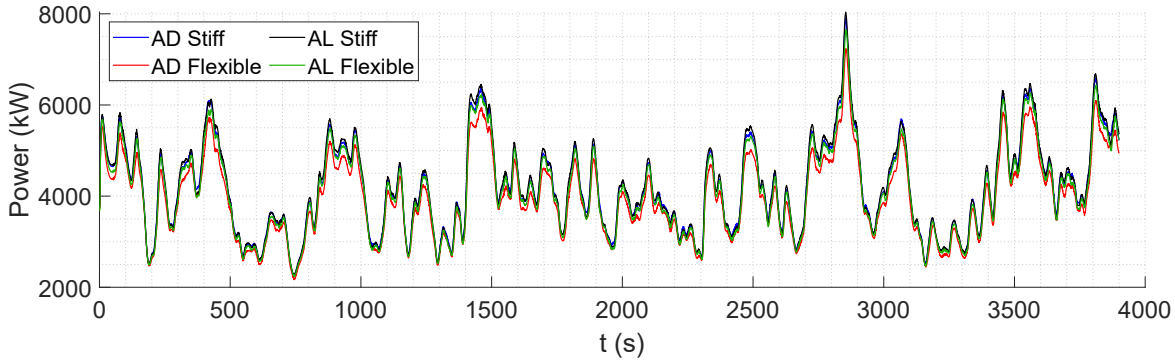

Figure 6. Power output against time for 8m/s

The stiff turbine results have an offset towards higher values; the mean power output is 5.6% and 2.7% greater for AD and AL respectively. This was also seen across other quantities investigated (pitch, thrust and torque) and suggests that including blade flexibility has a dampening effect, moderating the impact of fast controller changes. Between the flexible AL

and flexible AD, the largest differences can be seen at the power peaks, often reaching more than 6% higher in AL. The overall difference in mean power is 3.4%.

A further set of simulations (results not shown for brevity), were conducted with a grid twice as fine, at 32 mesh points per radius. The difference in mean power between the two flexible cases was reduced to less than 1%, and the choice of stiff or flexible turbine became the most important factor, rather than the flexible actuator disc appearing to be an outlier. However, the increased resolution also increases the angle of attack estimation error of the actuator line, related to the choice of smearing length ϵ [26]. The impact of the change in discretisation highlights the need to consider more challenging scenarios in grid studies. A 1% difference in CT was judged to be an acceptable uncertainty for the simple steady-state scenario, but this does not guarantee that higher variability and uncertainty will not arise in more complex flow cases. Additionally, this demonstrates the size of the uncertainties present, even for a relatively well-resolved turbine representation, and hence the risks in extrapolating conclusions from small percentage changes in mean quantities.

Another important aspect of turbulence for wind turbines is the fatigue of components. Figure 7 shows distributions of damage equivalent load (DEL) for flapwise and edgewise bending moments. DEL were calculated with a Wöhler coefficient of 10 at a frequency of 1Hz, using 600s sampling intervals overlapping by 300s, taken from 300s until 3900s (a total of 11 periods). The data for all blades are combined into a single distribution for each simulation.

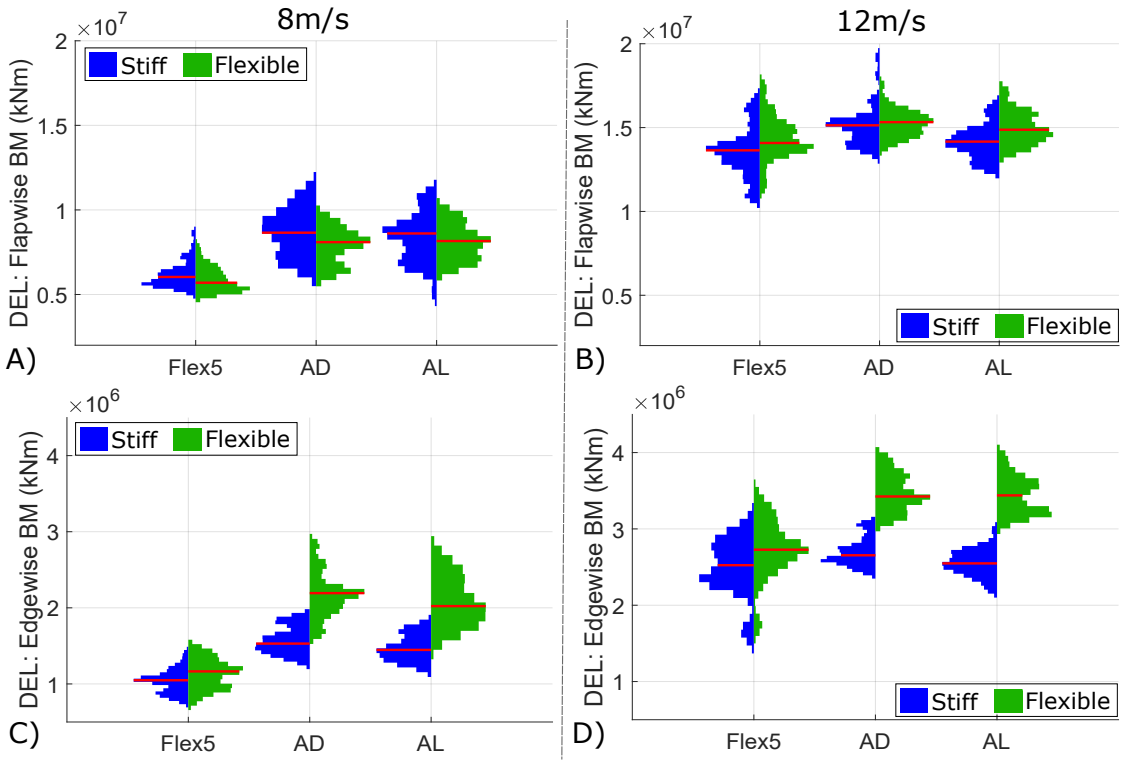

Figure 7. Damage Equivalent Load distributions: left- 8m/s; right- 12m/s; upper- flapwise bending moment; lower- edgewise bending moment. Median in red.

At 8m/s, Flex5 in standalone operation predicts much lower DEL than the coupled actuator methods, a reduction by around 25% and 45% for the flapwise and edgewise respectively (for the flexible turbine). Above rated, at 12m/s, the overall agreement between Flex5 and the actuator methods is improved, particularly for the flapwise bending moment. These differences reflect

the increased fidelity of the coupled simulations capturing the blade interaction with the flow, but also an overprediction of the blade tip and root loading, which could explain the better agreement above rated velocity. Accounting for flexibility in the coupled simulations causes a large increase in edgewise DEL, which is not seen in the flapwise DEL. The flapwise bending moment is governed by thrust, which (similar to Figure 5) shows good agreement between stiff and flexible. For the edgewise, with its smaller overall magnitude, the impact of tower flexibility may be more apparent. This is reflected in the edgewise bending moment time series (not presented here), which shows a larger magnitude of fluctuations for the flexible simulations.

For the coupled actuator methods, the choice of stiff or flexible turbine has a much more substantial impact than that of actuator disc or line. This is apparent when comparing both the median and distribution shape, which are well aligned when using the same turbine setup. Unlike in other results, the flexible actuator disc does not appear as an outlier from the other coupled actuator simulations.

5. Conclusion

The aim of this paper was to verify the coupling between the aeroelastic code Flex5, and the flow solver EllipSys3D which uses actuator methods to reduce the grid resolution required to model wind turbines. The intention of coupling these tools is to create a higher fidelity model framework than can be achieved just using a BEM-based aeroelastic solver, and hence this work also aimed to compare the methods and explain observed differences. The influence of flexibility can demonstrate this increase in fidelity: for standalone Flex5, it had almost no effect; for the actuator methods differences could be seen as the coupling allows the turbine to deflect within, and interact with, the flow. The comparison between stiff and flexible can be seen most clearly for the damage equivalent loads. In both median and spread, the distributions for the two actuator methods were very similar, while the choice of stiff or flexible had a substantial impact, particularly giving rise to large differences in the edgewise DEL. The comparatively high blade length and flexibility of the DTU10MW RWT are likely to contribute to the magnitude of the differences seen between flexible and stiff results. Across the steady-state performance curves and turbulent studies, and despite some differences due to the implementations of the two actuator methods, there is good agreement, hence verifying the coupling between Flex5 and EllipSys3D.

Further work will implement the new tip smearing correction [32, 33] in the coupling and study its impact. A valuable addition to validate the coupling would be a comparison with a fully resolved rotor simulation, as well as extending the verification to other flow conditions such as yaw and shear, where differences are likely to be most pronounced.

Acknowledgements

This work is partly funded by the European Union Horizon 2020 research and innovation program under grant agreement no. 861291 as part of the Train2Wind Marie Skłodowska-Curie Innovation Training Network (https://www.train2wind.eu/).

References

[1] Larsen G C, Madsen H A, Thomsen K and Larsen T J 2008 Wake meandering: A pragmatic approach. *Wind Energy* **11(4)**, 377–395

[2] Sørensen J N, Mikkelsen R F, Henningson D S, Ivanell S, Sarmast S and Andersen S J 2015 Simulation of wind turbine wakes using the actuator line technique. *Phil. Trans. R. Soc. A.* **373**

[3] Troldborg N 2009 Actuator Line Modeling of Wind Turbine Wakes. *PhD Thesis, Department of Wind Energy*, Technical University of Denmark.

[4] Andersen S J, Breton S-P, Witha B, Ivanell S and Sørensen J N 2020 Global trends in the performance of large wind farms based on high-fidelity simulations, *Wind Energ. Sci.* **5** 1689–1703

[5] Sørensen J N and Shen W Z 2002 Numerical modeling of wind turbine wakes. *Journal of Fluids Engineering, Transactions of the ASME* **124(2)** 393–399
[6] Troldborg N, Zahle F, Réthoré P-E and Sørensen N N 2015 Comparison of wind turbine wake properties in non-sheared inflow predicted by different computational fluid dynamics rotor models. *Wind Energ.2015* **18** 1239 - 1250
[7] Storey R C, Norris S E and Cater J E 2015 An actuator sector method for efficient transient wind turbine simulation, *Wind Energ.,* **18**, 699– 711
[8] Krüger S, Steinfeld G, Kraft M and Lukassen L 2020 Validation of a coupled atmospheric-aeroelastic model system for wind turbine power and load calculations. *Wind Energy Science Discussions, 1–36.*
[9] Ramos-García N, Sessarego M and Horcas S G 2020 Aero-hydro-servo-elastic coupling of a multi-body finite-element solver and a multi-fidelity vortex method. *Wind Energy* **24(5)**
[10] Sprague M A *et al.* 2020 ExaWind: A multifidelity modeling and simulation environment for wind energy. *J. Phys.: Conf. Ser.* **1452** 012071
[11] Andersen S J *et al.* 2017 Performance and Equivalent Loads of Wind Turbines in Large Wind Farms *J. Phys.: Conf. Ser.* **854** 012001
[12] Andersen S J 2014 Simulation and Prediction of Wakes and Wake Interaction in Wind Farms *PhD Thesis, Department of Wind Energy*, Technical University of Denmark
[13] Øye S 1996 Flex4 simulation of wind turbine dynamics. In *Proc. of 28th IEA Meeting of Experts Concerning State of the Art of Aeroelastic Codes for Wind Turbine Calculations*, Lyngby, Denmark, 11–12 April 1996. Lyngby, Denmark: Technical University of Denmark.
[14] Branlard E S P 2019 Flexible multibody dynamics using joint coordinates and the Rayleigh-Ritz approximation: The general framework behind and beyond Flex. *Wind Energy*, **22(7)**, 877–893.
[15] Shen W Z, Mikkelsen R, Sørensen J N and Bak C 2005 Tip loss corrections for wind turbine computations. *Wind Energy,* **8(4)**, 457–475.
[16] Michelsen J A 1992 Basis3D—a platform for development of multiblock PDE solvers. *Report AFM*, Technical University of Denmark, Lyngby, Denmark
[17] Sørensen N N 1995 General purpose flow solver applied to flow over hills. PhD thesis, Technical University of Denmark, Lyngby, Denmark.
[18] Strelets M 2001 Detached eddy simulation of massively separated flows. 39th AIAA Aerospace Sciences Meeting and Exhibit, Reno, NV, 2001; 1–19. AIAA Paper 2001-0879.
[19] Deardorff J W 1972: Numerical Investigation of Neutral and Unstable Planetary Boundary Layers. *J. Atmos. Sci.,* **29** 91–115.
[20] Mikkelsen R 2003 Actuator Disc Methods Applied to Wind Turbines. *PhD thesis, Mek dept, Technical University of Denmark*
[21] Heinz J C 2013 Partitioned Fluid-Structure Interaction for Full Rotor Computations Using CFD. PhD thesis, Technical University of Denmark, Lyngby, Denmark
[22] Bak C 2013 Description of the DTU 10 MW Reference Wind Turbine. DTU Wind Energy Report-I. 0092, Roskilde, Denmark, Technical University of Denmark
[23] Mann J 1994 The spatial structure of neutral atmospheric surface-layer turbulence. *J. Fluid Mech.* **273**, 141–168
[24] Mann J 1998 Wind field simulation. *Probab. Eng. Mech.* **13**, 269–282
[25] Gilling L, Sørensen N and Rethore P 2009 Imposing resolved turbulence by an actuator in a detached eddy simulation of an airfoil. *Proc. of EWEC 2009, Marseille, France, 16–19 March 2009.*
[26] Meyer Forsting A R and Troldborg N 2020 Generalised grid requirements minimizing the actuator line angle-ofattack error *J. Phys.: Conf. Ser.* **1618**, 052001
[27] Wu Y and Porté-Agel F 2011 Large-Eddy Simulation of Wind-Turbine Wakes: Evaluation of Turbine Parametrisations *Boundary-Layer Meteorology* **138(3)**
[28] Zhang M and Stevens R A J M 2020 Characterizing the Coherent Structures Within and Above Large Wind Farms *Boundary-Layer Meteorology* **174(1)**
[29] Andersen S J, Sørensen J N and Mikkelsen R F 2017 Turbulence and entrainment length scales in large wind farms *Phil. Trans. R. Soc. A.* **375**
[30] Meyer Forsting A R 2017 Modelling Wind Turbine Inflow: The Induction Zone. PhD thesis, Technical University of Denmark, Denmark
[31] Dağ K O and Sørensen J N 2020 A new tip correction for actuator line computations. *Wind Energy,* **23(2)**, 148–160
[32] Meyer Forsting A R, Pirrung G R and Ramos-García N 2019 A vortex-based tip/smearing correction for the actuator line. *Wind Energy Science,* **4(2)**, 369–383
[33] Meyer Forsting A R, Pirrung G R and Ramos-García N 2020 Brief communication: A fast vortex-based smearing correction for the actuator line, *Wind Energ. Sci.* **5**, 349–353,